



# Test of loaded and unloaded natural stone masonry walls exposed to fire

Duc Toan Pham · Elodie Donval · Nicolas Pinoteau · Pierre Pimienta ·  
Didier Pallix

Received: 25 November 2021 / Accepted: 3 October 2022 / Published online: 27 October 2022  
© The Author(s) 2022

**Abstract** This paper describes two full-scale tests carried out on two natural stone masonry walls subjected to fire loading, the first one was thermally loaded only (exposed to fire during 120 min without failure, then a natural cooling phase was observed) while the second one was thermally and mechanically loaded (exposed to fire and loaded up to failure with a compressive force at its bottom end). The experimental results showed that the thermal bowing was greatly affected by the in-plane mechanical loading. A water vaporization plateau at about 100 °C has also been observed, showing the influence of the hydric phenomena on the temperature distribution across the wall thickness. Analysis of cracking and failure of the walls showed that crack initiated in the vertical joints and propagated vertically through the blocks, which is quite typical for masonry in compression. Furthermore, the

observed fire behaviour of natural stone masonry walls has been compared to the fire behaviour of newer, manufactured materials such as hollow bricks, concrete blocks or reinforced concrete walls.

**Keywords** Masonry wall · Natural stone · Full scale test · Fire loading · Bearing wall

## 1 Introduction

While design methods for masonry structures at ambient temperature have been significantly improved during the past decades, this has not been the case for assessing the behaviour of a masonry wall in fire condition. As shown by Daware and Naser [1] in their extensive review about existing fire tests, the fire behaviour of masonry has begun to raise interest as early as the 1920's, with Ingberg's fire tests on brick walls (see Ingberg [2] for more details). Other experimental campaigns were conducted by Foster et al. ([3, 4]) on concrete masonry units in 1950. In 1979, another experimental campaign on the fire behaviour of extruded bricks was carried out by Byrne [5]. This campaign allowed to emphasise the thermal bowing phenomenon and its influence on the fire behaviour of the walls. In addition, Byrne notably showed that the slenderness of the wall had a negative impact on its fire resistance. However, a vertical compressive load might have either a positive

---

A1 D. T. Pham (✉) · E. Donval · N. Pinoteau · P. Pimienta  
A2 Centre Scientifique et Technique du Bâtiment (CSTB),  
A3 84 avenue Jean Jaurès, Champs-sur-Marne,  
A4 77447 Marne-la-Vallée Cedex 2, France  
A5 e-mail: ductoan.pham@cbstb.fr

A6 E. Donval  
A7 Laboratoire Navier (Ecole des Ponts ParisTech,  
A8 Université Gustave Eiffel, CNRS UMR 8205), 6-8 avenue  
A9 Blaise Pascal, Cité Descartes, Champs-sur-Marne,  
A10 77455 Marne-la-Vallée Cedex 2, France

A11 D. Pallix  
A12 Centre Technique de Matériaux Naturels de Construction,  
A13 17 rue Letellier, 75015 Paris, France



stabilising effect or a negative effect depending on its magnitude on the fire resistance of the wall.

Relatively recent experimental campaigns have been published with more details than previous works, both in terms of temperatures and in terms of displacements records. One may quote, among others, hollow clay bricks tested by Al Nahhas et al. [6] and Nguyen and Meftah [7]; hollow concrete blocks tested by Oliveira et al. [8] and Pope [9] or dry stacked blocks tested by Oliveira et al. [10]. All these experiments have emphasised the existence and the influence of thermal bowing, and its dependence to the geometrical characteristics of the wall, to the mechanical properties of the materials and to the loading level.

As experiments on full-size walls are voluminous and costly, other experiments have been conducted on masonry wallets by Russo and Sciarretta [11] on plain clay bricks and by Ayala [12] on lightweight aggregate blocks, allowing to study the influence of fire on the compressive resistance of the block-mortar assembly. Concerning natural stone masonry walls, test data on wallets or on full-size walls remains scarce and the literature is oriented towards real fires (see for example the work of Dionísio [13] on the post-fire decay of the cloister of Lisbon Cathedral or the recent work of Bertetto et al. [14] on the residual strength of Notre-Dame de Paris's stones). As a result, the structural behaviour of natural stone masonry walls and their associated failure mechanisms during a fire remain with little knowledge, and design methods for natural stone masonry walls are scarcely developed regarding their behaviour in fire condition.

From a regulatory point of view, the reference text for the design of masonry structures subjected to fire loading in Europe is Eurocode 6 Part 1-2 (EN 1996-1-2 [15]) which requires prescriptive standards for the different kind of buildings (housing, public buildings – ERP in the French regulation) regarding mechanical resistance, integrity and insulation in fire circumstances. Different design methods depending on the category of masonry (manufactured blocs or natural stone) have also been proposed in Eurocode 6 Part 1-2 (EN 1996-1-2 [15]). This is the case, for example, of clay and concrete blocks where both simplified and advanced design methods, as well as tabulated values, are available. However, unlike other types of masonry, there is no tabulated value for the design of natural stone masonry elements exposed to fire and simplified or advanced design methods are less straightforward.

Consequently, critical temperatures as low as about 300–400 °C are often considered for the design, and full-scale fire tests may be required, making the use of natural stone complex and not as competitive as other kinds of masonry regarding the structural fire design. This is all the more regrettable as knowledge of the thermo-mechanical properties of natural stone and mortar has progressed considerably in recent years. Sciarretta et al. [16] gathered thermal and mechanical properties of around 140 marbles, granites, sandstones and limestones coming from various parts of the world. Concerning their mechanical properties, these stones were tested either in elevated temperature state or in residual state. It has notably been shown that the post-fire compressive and tensile strength as well as the elastic modulus and the Poisson coefficient of stones tend to be reduced with the temperature increase, especially for the stones exposed to temperatures higher than 400 °C. Regarding the thermo-mechanical properties of mortar at high temperature, some experimental data may be found in Bamonte et al. [17] for ordinary cementitious mortars, in Fernandes Neto et al. [18] for cement-lime mortars, in Pachta et al. [19] and Bacci [20] for cement-lime and lime mortars. They notably showed that the flexural strength of the mortar decreased from about 400 °C, but the compressive strength of some mortars increased from about 200 °C to 600 °C. However, there is still an experimental knowledge gap on the behaviour of such structures, either at a wallette or at a wall level.

In this context, the CSTB (Centre Scientifique et Technique du Bâtiment) and the CTMNC (Centre Technique de Matériaux Naturels de Construction) in France, have launched a joint study in order to bring up some answers to help design methods evolve for natural stone masonry. The goal is to identify thermal deformed shapes and the associated failure modes of natural stone masonry walls subjected to fire loading. For that purpose, an experimental campaign has been conducted on two natural stone walls subjected to a conventional fire on one side (the first one was thermally loaded only while the second one was thermally and mechanically loaded with a compressive force at its bottom end). From experimental observations described in the present paper, the tests results may provide a useful data base for the validation of future design methods for natural stone structures exposed to fire loading.



## 2 Description of the tests

### 2.1 Characteristics of the test walls

The tests have been performed on two natural stone masonry walls in which blocks were composed of limestone from the Paris area and bounded by natural hydraulic lime mortar. Both walls were 2.92 m-wide, 2.97 m-high and 0.2 m-thick (Fig. 1). Their height/thickness ratio was approximately equal to 15, which is common for existing masonry walls and satisfied the dimensional recommendation of Eurocode 6 Part 1-2 (EN 1996-1-2 [15]) where the height/thickness ratio should be lower than 27.

The two walls were made of Saint-Vaast limestone blocks coming from Oise (France). Blocks' dimensions were 720 mm-long, 360 mm-high and 200 mm-thick. The density of the blocks was about 1640 kg/m<sup>3</sup>. The compressive strength of the limestone has been assessed following NF EN 772-1 [21] on 10 cubic 10 cm-side samples. Mean compressive strength was 7.4 MPa, with 0.34 MPa (5%) standard deviation. It should be noted that, in general, the material properties of natural stones can be quite fluctuating.

The walls were assembled by a “Compagnon du Devoir” (French expert craftsmanship organisation), according to running-bond pattern. The blocks were bonded by 10 mm hydraulic horizontal and vertical mortar joints. The mortar mix was 1:3 (volume of

NHL 3.5 lime:volume of sand) with natural hydraulic lime NHL 3.5 for the horizontal and vertical joints, as well as for the lower and upper screeds. This mix complies with the current French NF DTU 20.1 [22]. Due to experimental constraints, a 25-days curing period was archived for the unloaded wall while the curing period for the loaded wall was 29-days. This difference might have a small impact on the thermal transfer and on the compressive strength of the mortar.

### 2.2 Test setup

According to the NF EN 1363-1 norm [23], each wall was positioned inside a reinforced concrete (RC) frame for transportation (including retrieving the sample after the fire test) to place the test specimen in front of the furnace (see Fig. 2). For both walls, a 20 mm mortar screed bounded the bottom part of the wall and the RC frame. A 60 mm-wide rock wool strip (insulating material) was positioned between each vertical lateral side of the wall and the RC frame in order to ensure thermal insulation and prevent any thermal action on the lateral sides of the wall. The role of the concrete frame (with the sample inside) was also to close the furnace while exposing the test sample on one side.

The unloaded wall was positioned inside a closed RC frame while a mobile rigid beam was positioned on the top of the loaded wall. This mobile beam and the top of the loaded wall were bounded by a 67 mm mortar screed. A 40 mm gap was always ensured between the top beam and the concrete frame in order to allow for free thermal dilatation of the unloaded wall.

Both walls were exposed to a conventional ISO 834-1 fire (EN 1991-1-2 [24]) on one side. The first wall was not mechanically loaded in order to observe phenomena occurring during heating without failure due to a mechanical loading. The second wall was loaded with a vertical compressive load of 250 kN per linear metre over the width of the wall. The goal was to apply a sufficient load in order to observe failure modes of the wall during the second test. For illustrative purpose, Fig. 2 shows the test setup and implementation of the test on the loaded wall.

The gas furnace (see Fig. 2) enabled to apply a uniform thermal solicitation on the whole inner surface of the wall. Such a thermal solicitation followed the ISO 834-1 temperature curve (EN

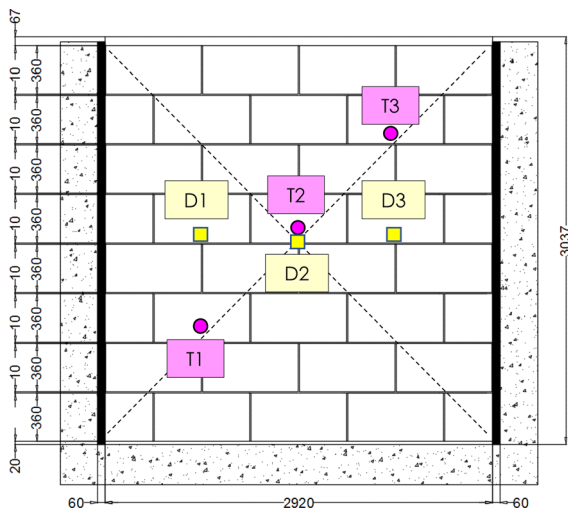


**Fig. 1** Dimensions of the test walls and arrangement of the blocks (with position of the thermocouples blocks (T1–T3) and of the LVDTs (D1–D3))

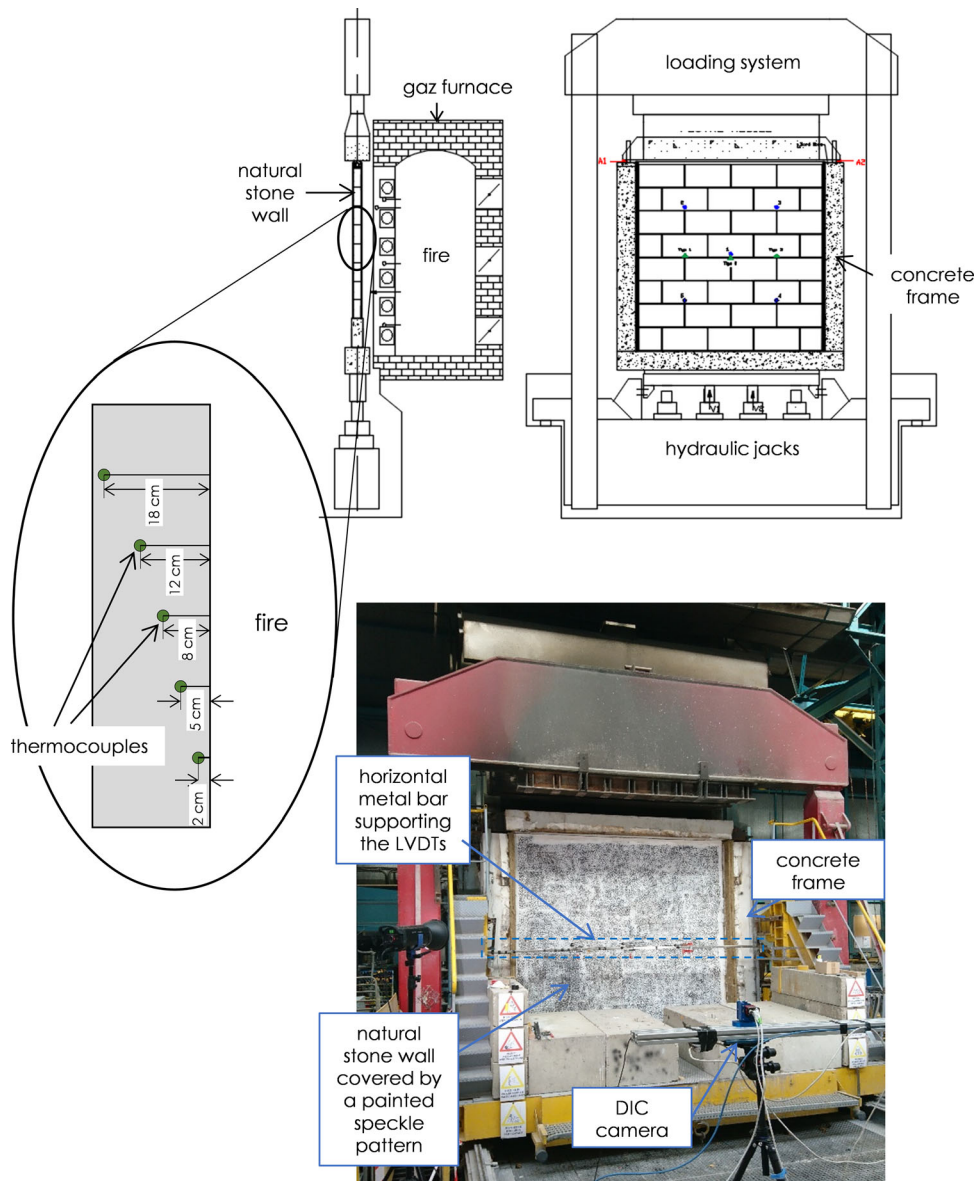


**Fig. 2** Test setup and implementation of a test

1991-1-2 [24]) and was applied during 120 min for the unloaded wall and up to failure of the loaded wall. It may be recalled that the ISO 834-1 curve was designed to model the hot gases temperatures during a flash-over where the increase in temperature is quick at the beginning (about 300 °C in 1 min). The temperature then reached 1000 to 1050 °C between 60 and 120 min of fire exposure. This thermal loading was controlled by using nine plate thermometers

positioned inside the furnace and at about 100 mm from the exposed surface of the test wall.

During the loaded test, the compressive load (of 250 kN/m) was applied by two hydraulic actuators acting on the rigid RC frame in order to uniformly distribute the load over the width of the wall (see Fig. 2). This compressive load was applied before the beginning of the fire and was maintained constant during the duration of the fire until the failure of the wall.

### 2.3 Instrumentation and measurements

During the two tests, temperatures and displacements of the wall were measured and recorded. The temperatures were measured by thermocouples positioned at different depths across the wall thickness (at 20, 50, 80, 120 and 180 mm from the exposed surface—see Fig. 2 for more details). These thermocouples were placed on three stone blocks (T1, T2 and T3) located in the diagonal of the wall as shown in Fig. 1. Thermal program was also monitored via plate thermocouples placed inside the furnace and burners were manually controlled to ensure that the prescribed temperature evolution followed the ISO 834-1 curve (EN 1991-1-2 [24]).

It should be noted that temperature in the mortar joints was not measured. Thermal properties of stone blocks and mortar joints were not measured, but some values of thermal conductivity and heat capacity of another lime stone and another lime mortar found in the literature are quite similar. Vigroux et al. [25] have reported a thermal conductivity  $\lambda = 1.1 \text{ W} \cdot \text{m}^{-1} \cdot \text{K}^{-1}$  and a heat capacity of  $C_p = 910 \text{ J} \cdot \text{kg}^{-1} \cdot ^\circ\text{C}^{-1}$  for Saint Maximin limestone while Masdeu et al. [26] have reported a thermal conductivity of  $\lambda = 0.7 \text{ W} \cdot \text{m}^{-1} \cdot \text{K}^{-1}$  and a heat capacity of  $C_p = 931 \text{ J} \cdot \text{kg}^{-1} \cdot ^\circ\text{C}^{-1}$  for a standard lime mortar. Considering that the thickness of the joints is very small compared to the blocks' height such as the case of the present tests, the temperature in the joints may be considered to be approximately the same as in the stone blocks.

The measurement of the displacement was performed by two different means: classical linear variable differential transformer sensors (LVDTs) and stereo Digital Image Correlation (DIC) technique. Three LVDTs (D1, D2 and D3) were fixed on a horizontal metal bar at mid-height of the wall and connected with its unexposed side in order to measure the horizontal out of plane displacements (see Figs. 1 and 2 for more details). The DIC system enabled to gather displacement fields in the three directions of the wall using two cameras, without any contact. For that purpose, the unexposed surface of the test sample was covered by a painted speckle pattern which enabled the system to determine the displacement of a set of points by comparing pictures taken at two different times. The position of the two cameras was calibrated before the test to be able to calculate displacements in

the three directions by triangulation. From these measures, it has been possible to determine, among others, the out-of-plane deflection of the wall.

## 3 Results of tests and discussions

The unloaded wall was exposed to fire during 120 min without failure, then a natural cooling phase was observed, while the loaded wall was exposed to fire up to failure. The failure of the latter wall was recorded after around 27 min of fire exposure.

### 3.1 Recorded temperatures

The ambient temperature at the beginning of the two tests was recorded with an average value around  $18^\circ\text{C}$ . The evolution of the furnace temperature in comparison with the ISO 834-1 curve (EN 1991-1-2 [24]), for both loaded and unloaded walls, is presented in Fig. 3, showing an overshoot in the early stages of the tests but the average temperature remained inside the limit tolerances of NF EN 1363-1 [23] after about 10 min.

Figure 4 presents the evolution of the temperature measured with thermocouples positioned at different depths across the thickness of the walls and the temperature evolution of their unexposed face. It can be seen that the evolution of the temperature tended to mark a plateau at around  $100^\circ\text{C}$ . This phenomenon, which can also be observed for cementitious materials, was due to the vaporisation of water within stone, which consumed part of the thermal energy received by the stone. This slowed the increase of temperature. It has also been shown that temperature of the unexposed face of the walls was maintained around ambient temperature for the first hour of fire exposure, then slowly increased and reached about  $65^\circ\text{C}$  after two hours for the case of unloaded wall (see Fig. 4).

Figure 5 shows the average temperature profiles in the thickness of the unloaded wall, for different fire exposures ranging from 30 to 120 min. It can be immediately seen that temperatures decreased quickly in the wall thickness. After 60 min of fire exposure, the temperatures of the three-quarters of the wall thickness (above the first 50 mm from the exposed side) were still lower than  $100^\circ\text{C}$  and temperature on the unexposed side was around  $18^\circ\text{C}$ . These thermal gradients might have a strong influence on the

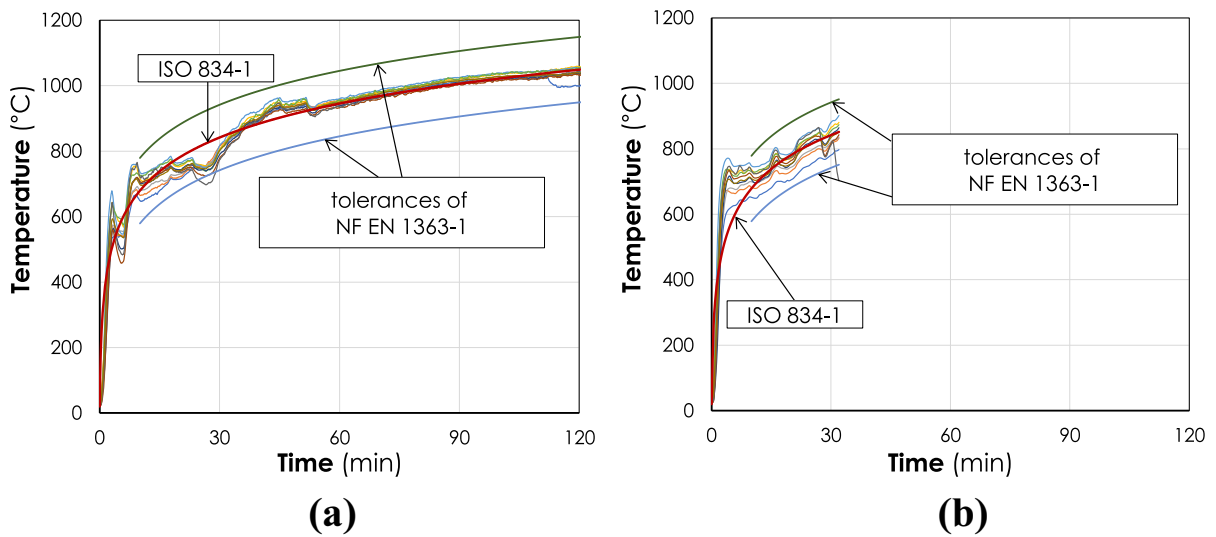


**Fig. 3** Evolution of the temperature measured inside the furnace for the test on **a** the unloaded wall and **b** the loaded wall

mechanical behaviour of the whole structure by inducing a thermal curvature of the tested specimen towards fire. At the same time, such an increase of temperature may also lead to a decrease of the stiffness and strength properties of the constituent materials.

### 3.2 Results of the unloaded test

#### 3.2.1 Deformed shape

When the wall was subjected to fire on one side, its exposed surface expanded more than its unexposed surface, resulting in a bending of the wall towards fire. During heating, the deformation of the unloaded wall was visible. Out-of-plane displacement fields (horizontal deflections) have been measured by LVDT sensors and the DIC technique at different fire exposures.

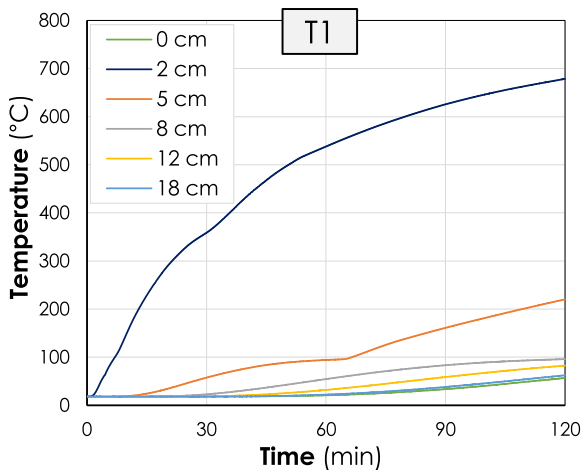
Figure 6 represents the evolution of the out-of-plane deflections measured by three LVDT sensors (D1–D3) as functions of fire exposure (from 0 to 120 min). It appears from this figure that thermal curvature developed both in the horizontal and in the vertical directions, hence creating a circular bulge towards the fire. The deflection at the centre of the wall evolved quickly at the beginning of the test and reached the value of 34 mm after 30 min of fire exposure. Then, the deflection increased slowly, and the increase of the deflection between 60 and 120 min

did not seem significant (around only 3 mm). In addition, the double thermal curvature (horizontal and vertical) was also outlined by the results of the DIC technique of which measurements were close to those obtained by LVDTs. Figure 7 shows the contours of the out-of-plane displacements (deflections) of the unloaded wall for different fire exposures, where the displacement towards fire has a negative value. It can be seen that the maximal deflection, at the centre of the wall, reached a value of 39 mm after 120 min of fire exposure. This represented almost about 20% of the wall thickness, (the wall being 200 mm-thick). In addition, Fig. 8 represents the deflection profiles along the height at mid-width as well as along the width at mid-height of the wall for different fire exposures. It can be seen that a double curvature of thermal bowing should be considered (which was not only along the vertical axis as often assumed when using 1D models (see Shields et al. [27] for example)).

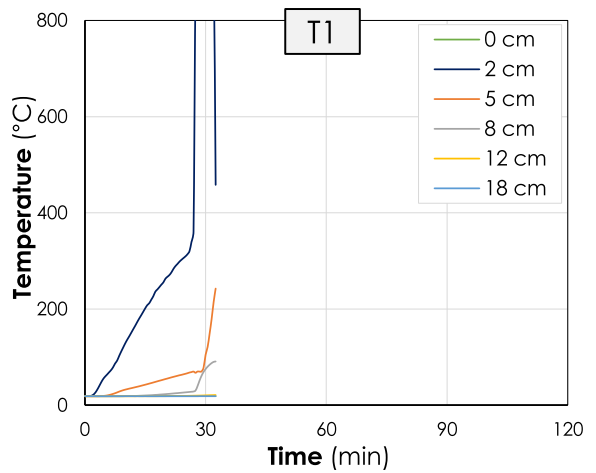
It is to note that DIC provides the displacement fields in the 3 directions. The LVDT (more traditional and recognised measurement) allows to compare these displacements at different points as shown in Fig. 8.

#### 3.2.2 Cracking

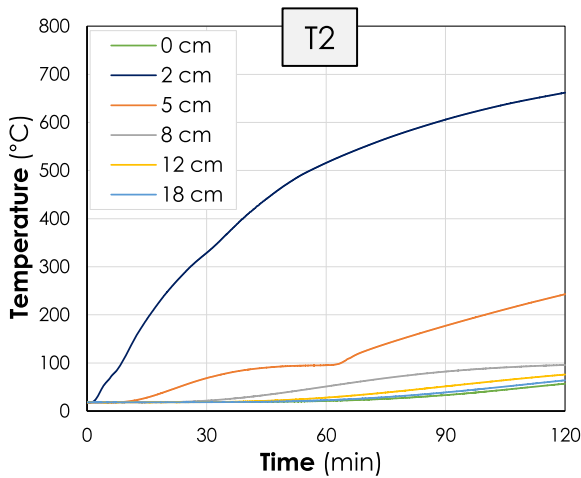
The use of the DIC technique also allowed observing the crack formation and evolution during the test. Indeed, cracks caused major local deformations, that



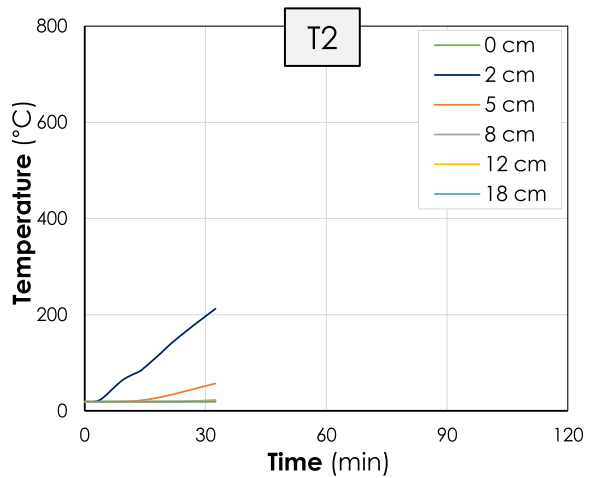
(a)



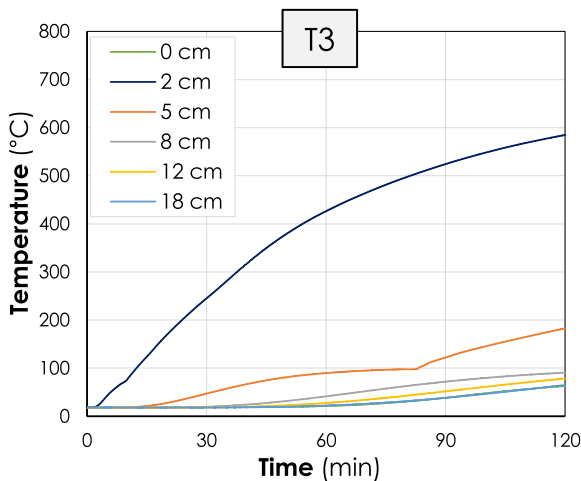
(b)



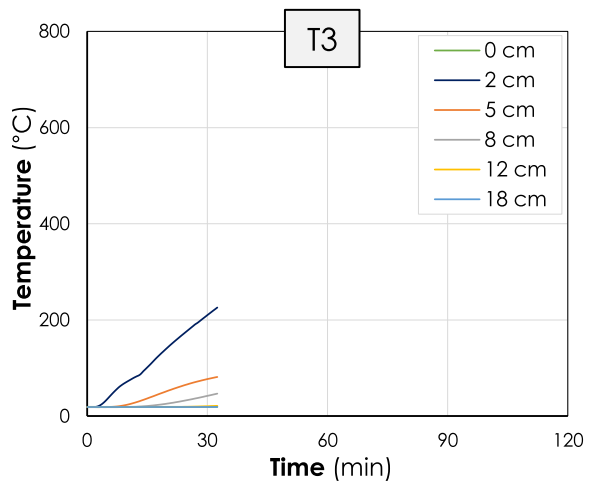
(c)



(d)



(e)



(f)

◀ **Fig. 4** Evolution of the temperature at different depths across the thickness at **a** T1, **b** T2 and **c** T3 of the unloaded wall and at **d** T1, **e** T2 and **f** T3 of the loaded wall

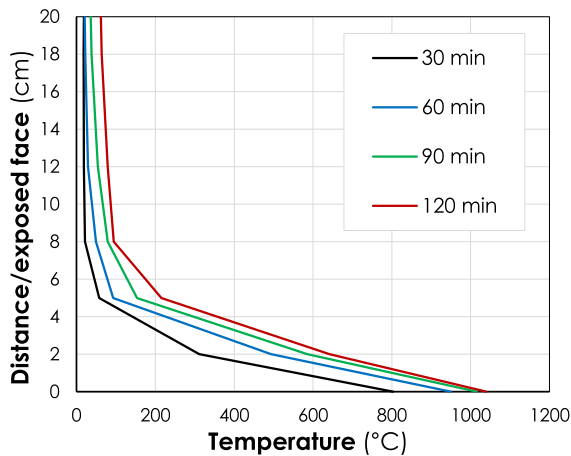


**Fig. 5** Average temperature distributions across the unloaded wall thickness for different fire exposures

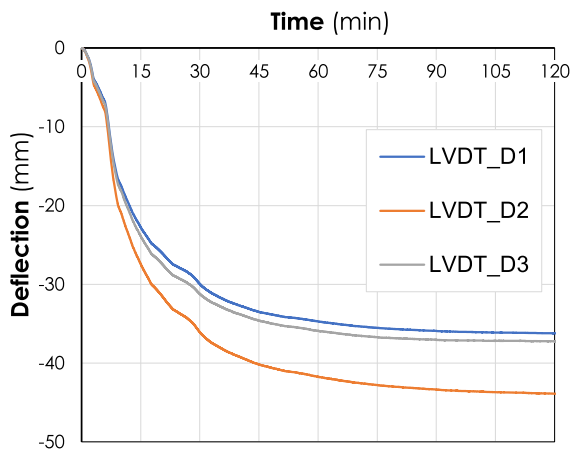


**Fig. 6** Evolution of the out-of-plane displacements at mid-high of the unloaded wall

can be obtained by spatial derivation of the displacement fields stemming from the DIC analysis (see Fig. 9). It was observed that most of the cracks initiated in vertical joints and propagated vertically through stones. Another observation was that these cracks did not seem to have significant influence on the thermal curvature of the wall. The thermal curvature seemed relatively continuous in both vertical and horizontal directions despite the presence of these cracks and the presence of two materials: mortar and

stone. The impact of the latter material might be low due to the fact that the thickness of the joints is very small compared to the blocks' height. In addition, the thermal expansion coefficient of these two materials were not measured and no value was found in the literature, but some values of thermal expansion coefficient of another lime stone and another lime mortar found in the literature are quite close. Indeed, mortars thermal expansion coefficients' values in the literature are around  $7\text{--}10 \times 10^{-6}/^{\circ}\text{C}$  (see Zeng et al. [28], Santhanam et Ramadoss [29] for example) at ambient temperature, while the thermal expansion coefficient of limestone at ambient temperature is around  $5 \times 10^{-6}/^{\circ}\text{C}$  (see Vigroux [30] for more details). At the end of the test, a crack along the width of the wall, under the first bed of blocks, was also observed. Cracks on the un-exposed as well as on the exposed surface of the wall after the test are shown in Fig. 10.

### 3.2.3 Cooling of the wall

The deflection was also measured after the test during a 100 min cooling of the wall. Figure 11a represents the evolution of the temperature within the wall during the cooling phase, while Fig. 11b represents the evolution of the out-of-plane horizontal displacement at the same time. As it can be observed on the thermal profile, the thermal inertia of natural stone is high. The temperature of the unexposed face of the wall kept increasing during 60 min after the end of the test. At 100 min after the end of the test, the temperature was still higher than  $100^{\circ}\text{C}$  at 120 mm from the exposed face of the wall.

In addition, as shown in Fig. 11b, during the cooling the wall progressively unbended with displacements opposite to the heating face. This was due to the progressive decrease of the thermal gradient (Fig. 11a). After 100 min of cooling, the maximal deflection reached 29 mm, which represents about 65% of the maximal deflection after 120 min of fire exposure and about 15% of the thickness of the wall. In this case, irreversible out-of-plane displacement would be due to inelastic and irreversible deformation coming both from the thermal and mechanical loadings, as well as irreversible chemical transformations. One can cite, for instance, decarbonation of calcite and lime and portlandite formation that occur from about  $700^{\circ}\text{C}$  in calcareous stones. Such an irreversible



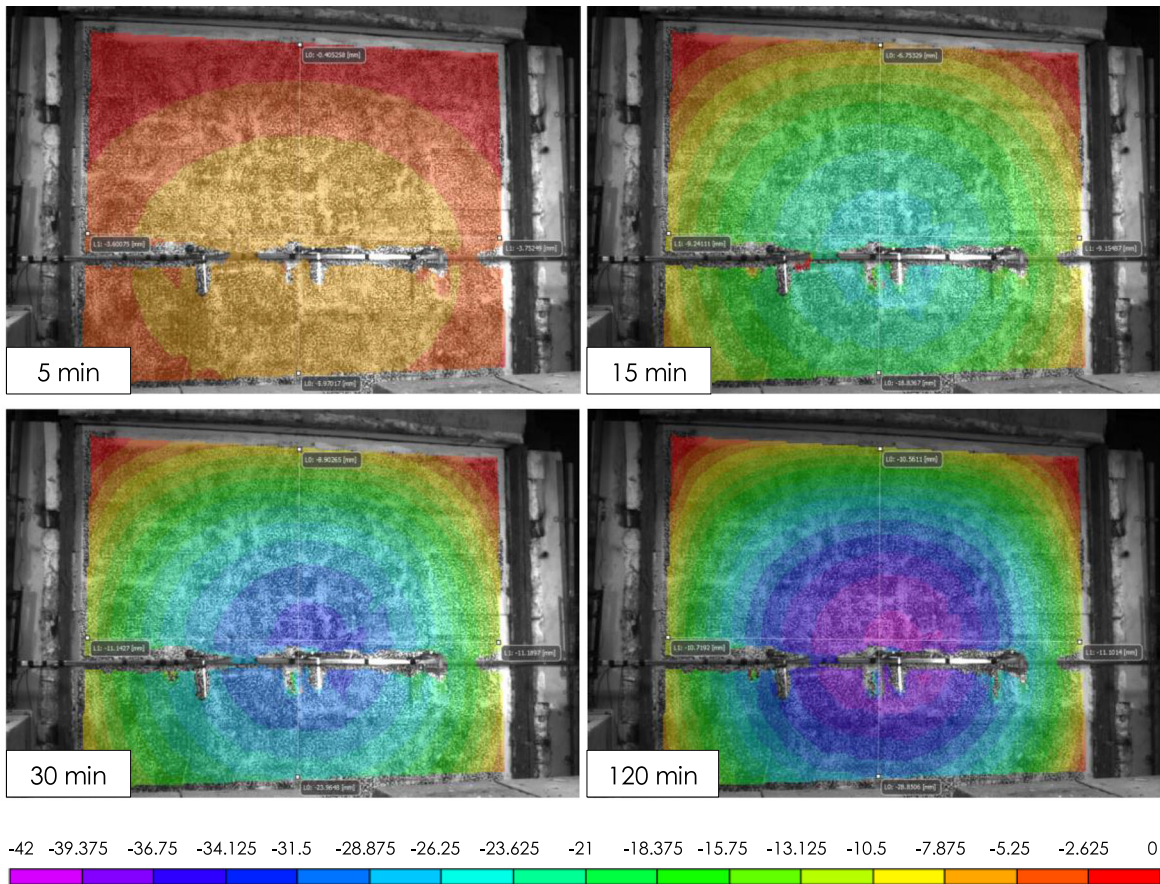


**Fig. 7** Contours of the out-of-plane displacements of the unloaded wall for different fire exposures

behaviour is not specific to masonry and can also be observed for concrete as shown in Pham et al. [31] for instance.

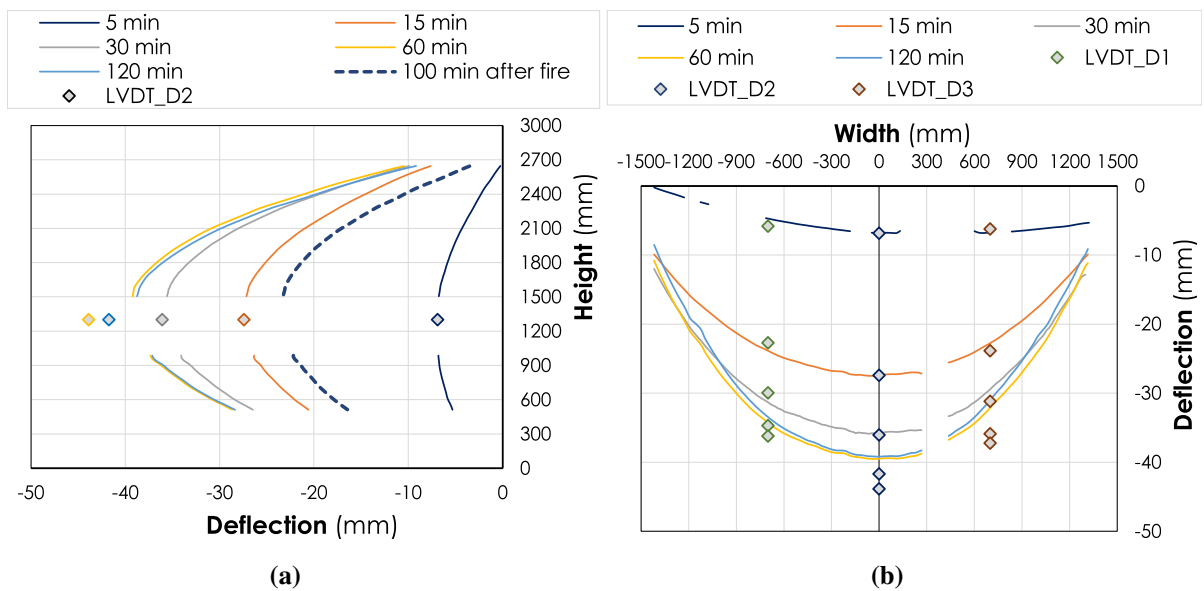
### 3.2.4 Post-fire crack

Figure 10 shows the post-fire patterns of the exposed face of the wall. Some vertical cracks that were noticed by the DIC system on the unexposed face can also be observed on the exposed face. It can be noticed that a network of superficial cracks appeared on the surface. Such a phenomenon has already been documented by several authors, in particular Vigroux [30] for limestone from the Paris area exposed to high temperatures up to 800 °C. This superficial cracking was mainly due to lime rehydration and occurred in the 24 h following the heating of the specimen. It only concerned the part of the stone in which the temperature has exceeded about 700 °C (first two centimetres

from the exposed face of the wall, i.e. 10% of the wall thickness). A change in colour, due the formation of portlandite from 700 °C, can also be observed: the surface of the wall, initially beige, has lightened and turned white.

### 3.3 Results of the loaded test

From a structural point of view, failure of the wall may be defined by the inability to sustain the vertical load applied on the wall. According to NF EN 1363-1 [23], this happens when the vertical sensor measuring the relative displacement between the concrete frame and the top beam recorded a contraction higher than 30 mm or a contraction rate higher than 9 mm/min. Such a failure was recorded after about 27 min for the loaded wall.



**Fig. 8** Deflection profiles **a** along the height at mid-width and **b** along the width at mid-height of the unloaded wall for different fire exposures

### 3.3.1 Cracking

The complete collapse of this wall happened short after the gas burners stopped (Fig. 12). For this test, more pronounced vertical cracks began to develop from about 10 min after the beginning of fire (corresponding to temperatures around 700 °C inside the furnace). Like the unloaded wall, the evolution of these cracks may be highlighted by the principal deformations' distributions obtained from DIC analysis, such as those shown in Fig. 12. It can be seen that a first crack appeared on the left side of the wall. After about 20 min of fire exposure, this crack has spread upside and downside, crossing blocks and through joints. In the meantime, other less pronounced vertical cracks developed. Firstly, a vertical crack developed in the right side of the wall, symmetrically to the one of the left side. Then, just before the failure of the wall, vertical cracks appeared in the centre of the wall.

### 3.3.2 Out-of-plane displacement

Unlike for the unloaded test, a major consequence of the aforementioned cracks was that thermal bowing of the loaded wall was not centred anymore (Fig. 13). Thermal bowing was significantly reduced compared to the one of the unloaded test. Indeed, the maximal

deflection reached only 5 mm after about 27 min of fire exposure, which represents only 2.5% of the thickness of the wall. The deflection profiles along the height at mid-width of the wall for different fire exposures has been shown in Fig. 13. It can be observed that the maximal deflection was not obtained at mid-height of the wall like for the unloaded wall but a bit higher, around 5/8th of the height. Such a phenomenon has already been reported in Al Nahhas et al. [6] and Nguyen and Meftah [7] for hollow blocks masonry walls. Besides, other experimental studies on normal height RC walls have also shown that a compressive load can limit thermal bowing (see Miah et al. [32] for example). It seems to be the case here, as at the beginning of heating (about 5 min) and before any appearance of cracking, the deflection of the loaded wall was about three times lower than the deflection of the unloaded wall.

### 3.3.3 Local and global failure mechanisms

Regular acquisition from the DIC system (one picture every six seconds) allowed to see two local failures concomitant to the collapse of the wall: a major vertical crack appeared on the right side of the wall, and a block in the second row split in the plan of the wall and broke down. However, no significant out-of-

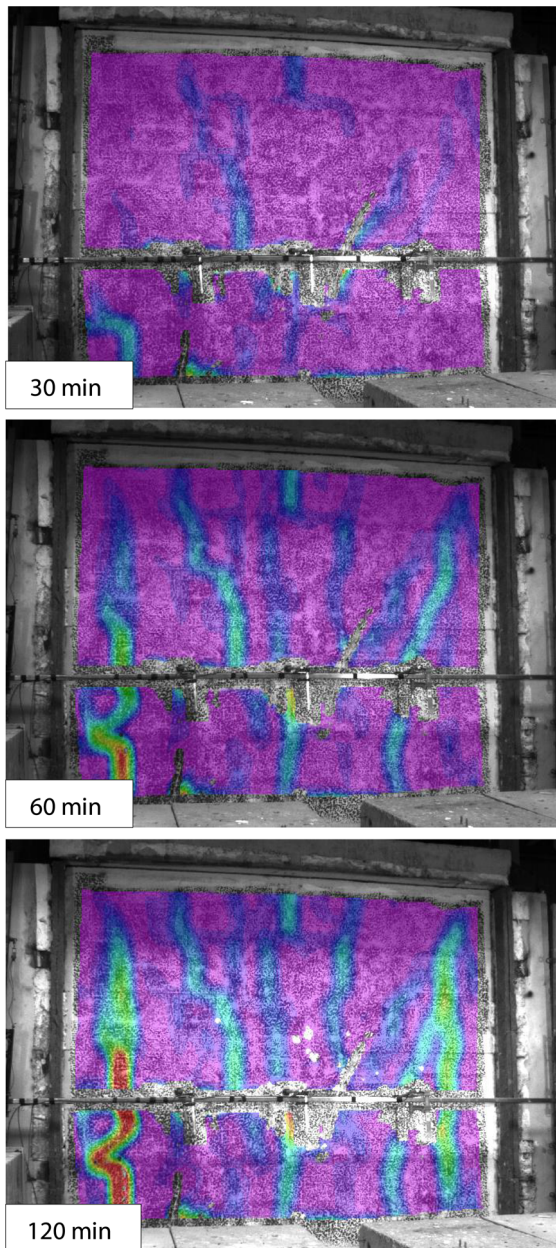


**Fig. 9** Cracking of the unloaded wall for different fire exposures (measured by DIC)

plane global movement of the wall was recorded at failure (Fig. 14).

From that moment, the load applied on the wall was 95 kN/m. About seven minutes after the structural failure, a major crack appeared and other blocks from the second and third row delaminated. Both vertical cracks and failure by splitting of the blocks tended to

indicate that the wall failed in compression. The full collapse of the wall occurred when moving the wall away from the furnace (Fig. 14), by chain effect: adjacent blocks failed progressively.

It has been shown that the compressive strength of limestone is usually barely altered by temperatures higher than 400 °C (Vigroux et al. [25], Sciarretta et al. [16]). At failure, the thermal profile (Fig. 5) shows that the temperature exceeded this value in less than 2 cm from the exposed face of the wall, so the compressive strength of the stone remained hardly unaffected in more than 90% of the thickness of the wall. Considering the 2 cm-part of the wall that might have been damaged by fire, the sole local decrease of the strength of limestone did not seem to be sufficient to explain the failure of the wall. Such a failure of the wall may probably be related to:

- Eccentricity of the load. The thermal bowing of the wall created an eccentricity of the vertical load with respect to the initial vertical plan of the wall and induced bending moments that added to the initial compressive forces. These additional bending moments, combined with the degradation of the materials, might trigger the failure of the wall.
- Material loss on the exposed side of the wall. The endoscopic camera allowed to see the delamination of around 2–3 cm of stone on the lower part of the wall concomitantly to failure. This led to a loss of about 10–15% of the thickness (and therefore of the compressive strength) of the wall.
- Variability of the properties of the materials. A failure due to a local default cannot be excluded.

#### 4 Discussion and comparison to other fire tests

The fire behaviour of natural stone masonry can be compared to the fire behaviour of newer, manufactured materials such as hollow bricks, concrete blocks or RC walls. The experimental results determined in this study can be compared with results found in the literature and determined on different types of masonry. In order to be able to carry out a direct comparative study, we have chosen to compare our results with those determined on masonry of the same thickness (thermal transfer comparison) and the same height (thermo mechanical and out of plane deflection comparison) such as the works of Nguyen and Meftah



**Fig. 10** Cracks on the exposed et un-exposed surface of the unloaded wall after the test

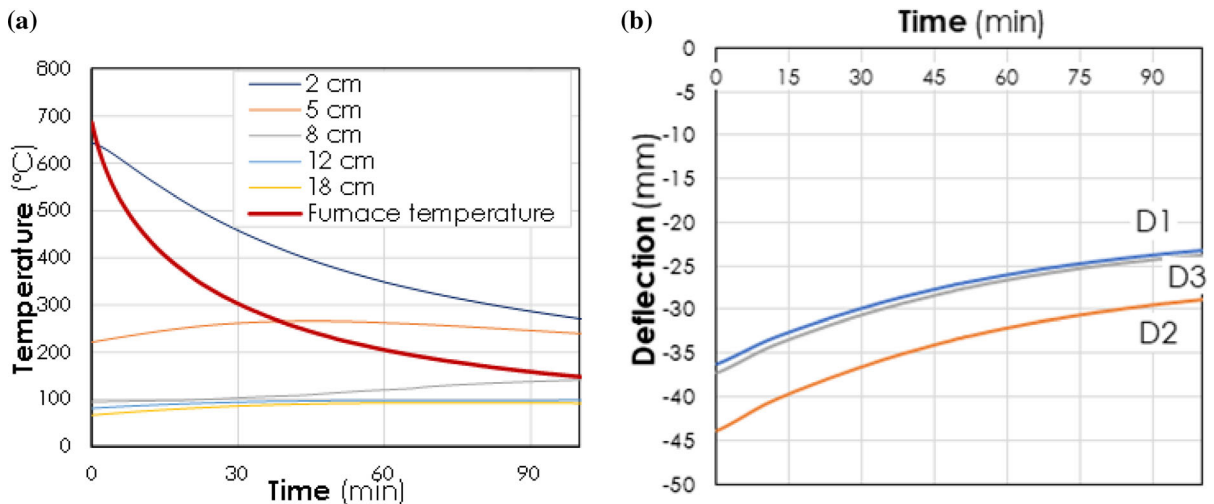


**Fig. 11** a Temperature distribution and b evolution of the out-of-plane displacement during the cooling phase

[7], Al Nahhas et al. [6] for bricks and Miah et al. [32] for RC walls.

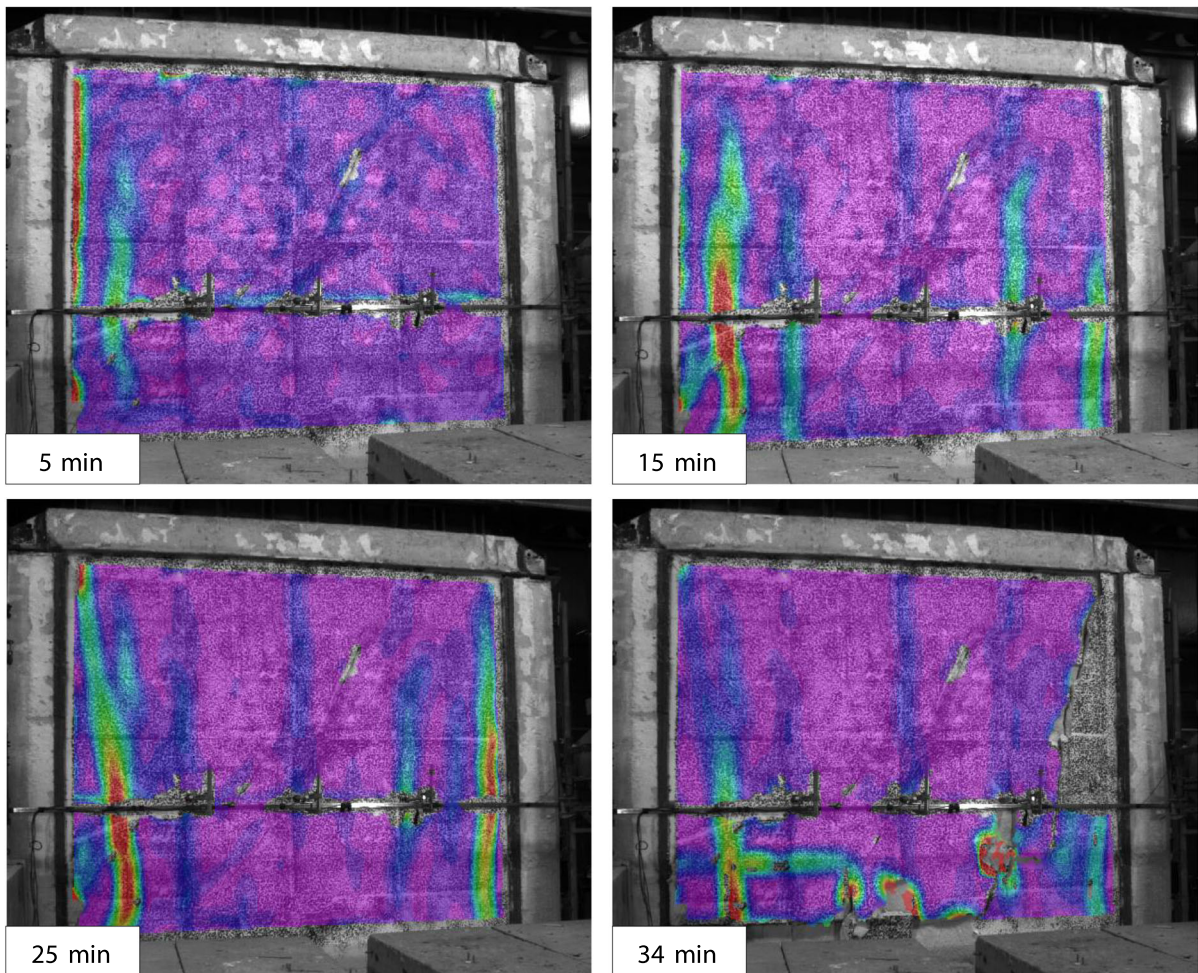
#### 4.1 Heat transfer

Figure 15 represents the temperature distribution in a RC wall without spalling (from Miah et al. [32]) and the Saint-Vaast limestone wall from this study. A thermal transfer calculation (using the FEM software SAFIR [33]) for a RC wall, following the ISO 834-1 fire curve (EN 1991-1-2 [24]) regarding fire-related boundary conditions, and EN 1992-1-2 [34] regarding the evolution of thermal properties of concrete (assumed to be made of calcareous aggregate and with a zero water content), has been added to Fig. 15 for comparative purpose. From this graph, it appears that natural stone is more isolating than concrete.

It may be interesting to note that the insulation criterion I (defined by the time during which the mean temperature of the unexposed face stays under 140 °C, and its maximal temperature stays under 180 °C—see EN 1992-1-2 [34] for more details) was exceeded at about 105 min for the hollow brick wall (due to the spalling and local failure of the hollow brick—see Nguyen and Meftah [7] for more details), while it was not exceeded during the test neither for the concrete wall nor for the unloaded natural stone wall.

#### 4.2 Influence of the mechanical load on the thermal bowing

The present experimental campaign showed that, for the walls considered, increasing the load from self-weight to 250 kN/m (73.3% of the preliminary prediction of the limit load at ambient temperature according to Eurocode 6 Part 1-1 (EN 1996-1-1 [35])—(see Appendix for the preliminary calculation) reduced significantly the out-of-plane displacement of the wall. This could be partially explained by the decrease of the Young modulus of the materials as a function of the temperature increase (see Vigroux [30] for example), which may make the exposed side of the wall less stiff. As a result, the mechanical neutral axis of the wall shifted towards the unexposed face. The load, initially centred, became off-centred and created additional bending moments that reduced the total curvature and out-of-plane displacement. Such a phenomenon has already been documented for RC walls by Miah et al. [32], who have shown experimentally that the out-of-plane horizontal deflection of highly loaded RC walls was significantly lower than the deflection of unloaded RC walls. In addition to the differential loss of stiffness, cracking, creep and potential transient thermal strains may explain this smaller out-of-plane displacement when the wall was highly loaded. Concerning brick masonry, Byrne [5] also showed experimentally that the thermal out-of-plane deflection was lower for highly loaded walls (about 100–125% of the limit load at ambient



**Fig. 12** Cracking measured by DIC for the loaded wall for different fire exposures

temperature according to the Australian Standard predictions) than for walls subjected to lower loadings (about 40–50% of the limit load at ambient temperature). Hence it seems that a vertical compressive loading may have a beneficial influence on the deformed shape of normal height natural stone masonry walls, but it may not be the case for their final fire resistance.

## 5 Conclusion

The two tests presented in this paper have provided first experimental data on the fire behaviour of natural stone masonry walls. They revealed some phenomena already observed for other kinds of masonry, such as

thermal bowing. Regarding the thermal observations, natural stone masonry has shown good performances in fire condition. Water vaporization at about 100 °C have also been observed, showing the influence of the hydric phenomena, especially moisture transfer, on the temperature distribution across the wall thickness.

A major observation was that natural stone masonry was concerned by thermal bowing, as other kinds of masonries. This thermal bowing was observed by the joint use of a DIC system and classical LVDT sensors. The use of both systems enabled to have a real-time image of the out-of-plane deflection on most of the wall by the DIC and on the sides (not observable by the DIC) by the LVDT sensors. The thermal bowing was greatly affected by the in-plane mechanical loading: the out-of-plane deflection was significantly lower for

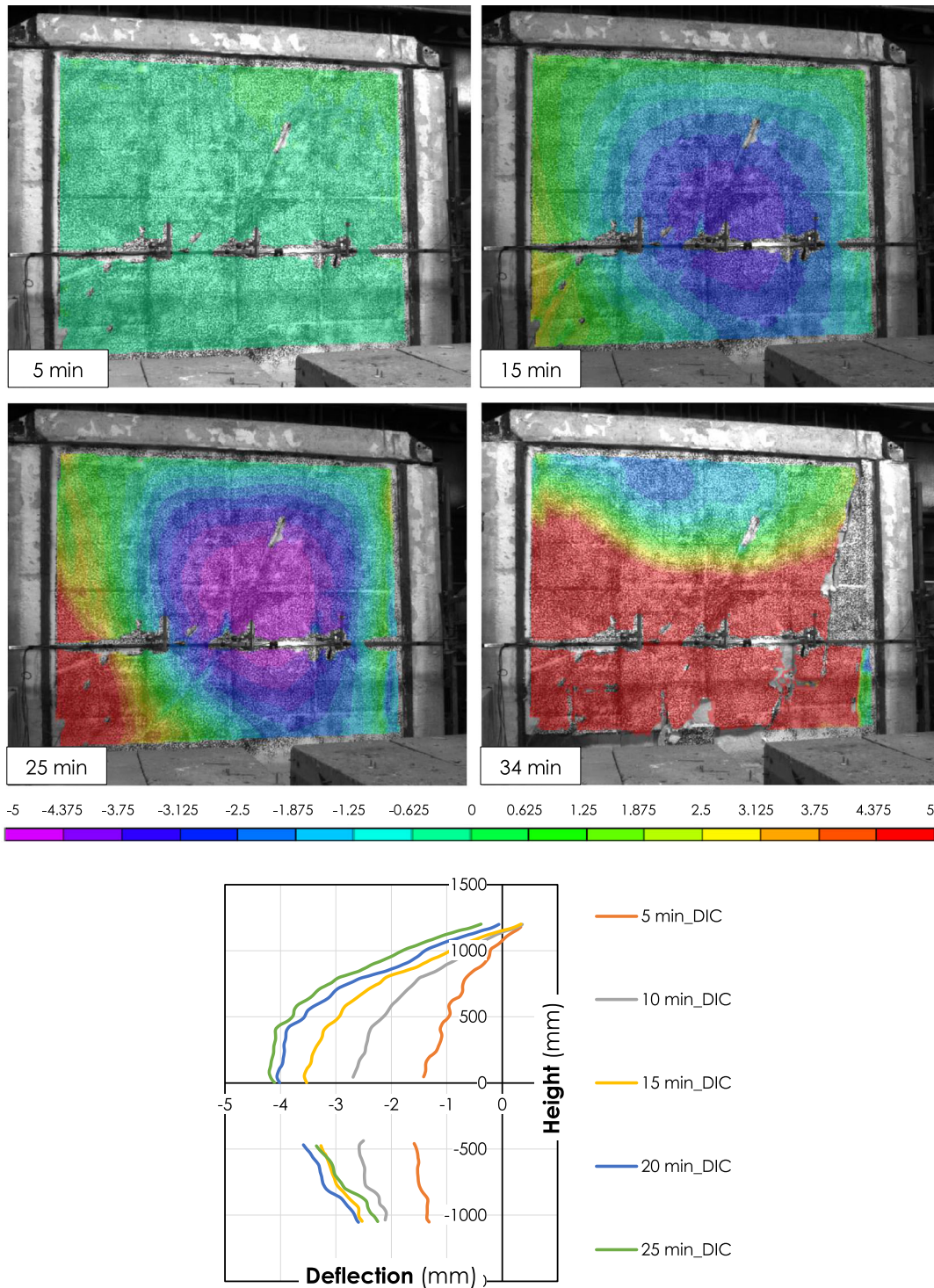


**Fig. 13** Contours of the out-of-plane displacements and deflection profiles along the height at mid-width of the loaded wall for different fire exposures

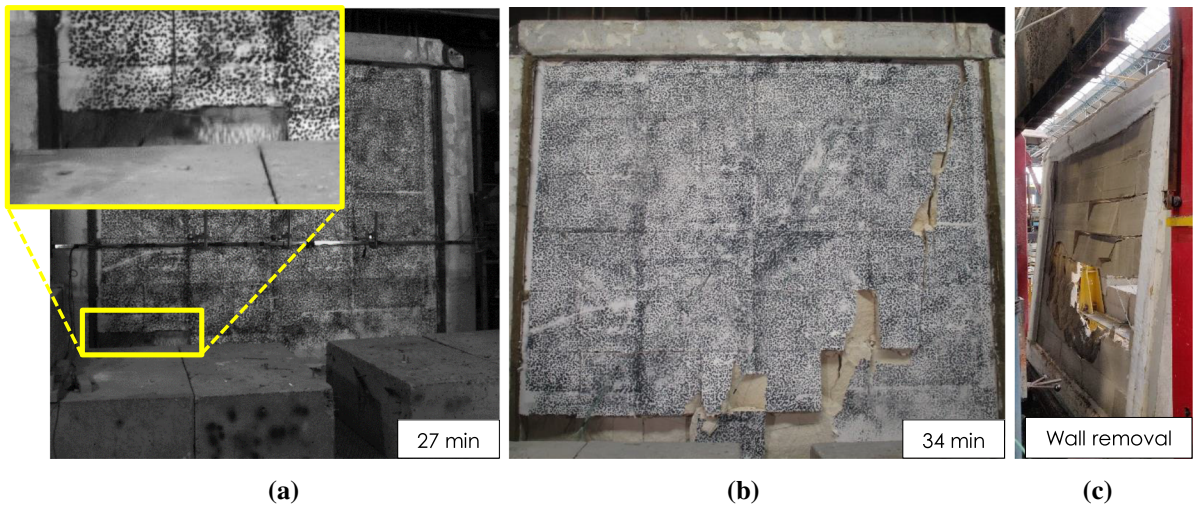


**Fig. 14** Progressive failure of the loaded wall: **a** splitting of a block, **b** major crack about 7 min after the extinction of gas burners, **c** superficial material loss observed when removing the wall

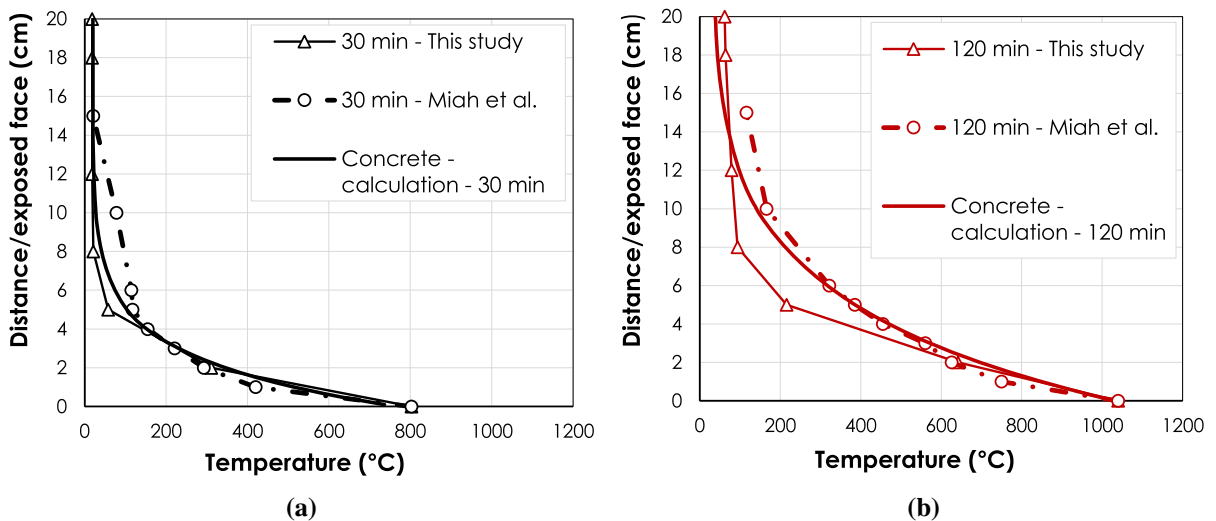


**Fig. 15** Thermal gradient for different walls exposed to an ISO 834-1 fire during **a** 30 min and **b** 120 min

the loaded wall than for the unloaded wall. Measures have also shown that the thermal curvature was partially reversible. As the cooling time was not long enough for the wall to come back to ambient temperature, it was not possible to observe whether the thermal curvature was entirely reversible or not. Given the occurrence of irreversible chemical phenomena and damage, the thermal bowing might be only partially reversible.

Concerning cracking and failure, the DIC system showed that crack initiated in the vertical joints and

propagated vertically through the blocks, which is quite typical for masonry in compression. This was confirmed by the failure mode: an in-plane splitting of blocks. However, the influence the thermal bowing and of the resulting eccentric vertical load with respect to the initial vertical plan of the wall may need to be taken into account.

In addition, this preliminary experimental study has also raised some questions and research needs:

- The lack of thermal and mechanical properties of mortar. Although the literature seems to be



increasingly growing on stone properties, it seems to be scarcer on mortar properties (Young modulus and thermal expansion coefficient for instance).

- The influence of the mechanical loading on the out-of-plane thermal deflection. It has already been investigated by several authors for other materials and may be completed by other tests on natural stone masonry walls (with other loads for example).
- Some hypotheses have been proposed to explain the early collapse of the wall, but additional theoretical and numerical investigations could bring other clarifications and explanations.

A further perspective of this study may concern the development of calculation methods for the fire behaviour of natural stone masonry walls, taking into account both the degradation of the materials due to the temperature increase and the effect of the thermal bowing.

**Acknowledgements** Authors wish to thank Mr. Stéphane Charuel, Mr. Léo Gontier and all the members of the experimental team of the Fire Studies and Tests Division at the CSTB for their help to make the tests successful. Much gratitude is expressed towards Mr. Philippe Leblond of the CSTB for guiding the initial development of the experimental program. We also thank Ms. Carla Pani of Rocamat, for kindly answering our questions about the physical and mechanical characteristics of the stones.

#### Declarations

**Conflict of interest** The authors declare that they have no conflict of interest.

#### Appendix

A preliminary estimation of the strength (by unit length) of a natural stone masonry wall at ambient temperature,  $N_R$ , may be carried out according to EN 1996-1-1 [35] as follows:

$$N_R = \phi_i \times t \times f \quad (1)$$

where:

- $\phi_i$  is a reduction factor that accounts for geometric imperfection, buckling risk and transversal horizontal loading when applicable. Here, it is lower at mid-height of the wall ( $\phi_i = 0.74$ ) than at its extremities ( $\phi_i = 0.9$ ).

- $t = 0.2$  m is the thickness of the wall;
- $f$  is the local strength of the block/mortar assembly, empirically determined by:

$$f = K \times f_b^{0.7} \times f_m^{0.3} \quad (2)$$

where:

- $K = 0.45$  for natural stone;
- $f_b = 7.4$  MPa is the compressive strength of stone;
- $f_m = 2.5$  MPa is the compressive strength of mortar used in this calculation (as a mortar class M2.5 is required for soft stones).

Here, the limit load of the wall, without taking into account partial safety factors, is  $N_R = 341$  kN/ml. A 250 kN/ml load corresponds to 73.3% of this empirical limit load at ambient temperature.

#### References

1. Daware A, Naser MZ (2021) Fire performance of masonry under various testing methods. *Constr Build Mater* 289:123183
2. Ingberg SH (1954) Fire tests of brick walls. U.S. Department of Commerce, Gaithersburg
3. Foster HD, Pinkston ER, Ingberg SH (1950) fire resistance of walls of lightweight-aggregate concrete masonry units. U.S. Department of Commerce, Gaithersburg
4. Foster HD, Pinkston ER, Ingberg SH (1951) Fire resistance of walls of gravel aggregate concrete masonry units. National Bureau of Standards, Gaithersburg
5. Byrne SM (1979) Fire resistance of load-bearing masonry walls. *Fire Technol* 15:180–188
6. Al NF, Ami SR, Bonnet G, Delmotte P (2007) Resistance to fire of walls constituted by hollow blocks: experiments and thermal modelling. *Appl Therm Eng* 27(1):258–267
7. Nguyen T-D, Meftah F (2012) Behavior of clay hollow-brick masonry walls during fire. Part 1: experimental analysis. *Fire Saf J* 52:55–64
8. Oliveira RG, Rodrigues JPC, Miguel PJ, Lourenço PB, Lopes RFR (2021) Experimental and numerical analysis on the structural fire behaviour of three-cell hollowed concrete masonry walls. *Eng Struct* 228:111439
9. Pope H (2021) Improving the fire resistance of concrete masonry walls. Ph.D. Thesis, Carleton University, Ottawa
10. Oliveira RLG, Rodrigues JPC, Pereira JM, Lourenço PB, Marschall HU (2021) Thermomechanical behaviour of refractory dry-stacked masonry walls under uniaxial compression. *Eng Struct* 240:112361
11. Russo S, Sciarretta F (2012) Experimental and theoretical investigation on masonry after high temperature exposure. *Exp Mech* 52(4):341–359



12. Ayala FRR (2011) Mechanical properties and structural behaviour of masonry at elevated temperatures. PhD Thesis, University of Manchester, Manchester
13. Dionísio A (2007) Stone decay induced by fire on historic buildings: the case of the cloister of Lisbon Cathedral (Portugal). *Geol Soc Lond Spec Publ* 271:87–98
14. Bertetto AM, D'Angella P, Fronterre M. (2021) Residual strength evaluation of Notre Dame surviving masonry after the fire. *Eng Fail Anal* 122:105183
15. EN 1996-1-2 (2005) Eurocode 6: design of masonry structures. Part 1-2: general rules-structural fire design
16. Sciarretta F, Eslami J, Beaucour A-L, Noumowé A (2021) State-of-the-art of construction stones for masonry exposed to high temperatures. *Constr Build Mater* 304:124536
17. Bamonte P, Gambarova PG, Sciarretta F (2021) Thermo-mechanical properties and stress-strain curves of ordinary cementitious mortars at elevated temperatures. *Constr Build Mater* 267:121027
18. Neto JADF, Sombra TN, Haach VG, Corrêa MRS (2022) Effects of post-fire curing on the residual mechanical behavior of cement-lime masonry mortars. *Constr Build Mater* 327:126613
19. Pachta V, Triantafyllaki S, Stefanidou M (2018) Performance of lime-based mortars at elevated temperatures. *Constr Build Mater* 189:576–584
20. Bacci J (2021) The influence of fire and water on lime, natural hydraulic lime, and cement-lime mortars. Mc.S Thesis, University of Pennsylvania, Pennsylvania
21. NF EN 772-1 (2015) Methods of test for masonry units-Part 1: determination of compressive strength
22. NF DTU 20.1. (2020) Ouvrages en maçonnerie de petits éléments-Parois et murs. (in French)
23. NF EN 1363-1 (2020) Essais de résistance au feu-Partie 1: exigences générales. (in French)
24. EN 1991-1-2 (2002) Eurocode 1: action on structures-Part 1-2: general actions. Actions on structures exposed to fire
25. Vigroux M, Eslami J, Beaucour A-L, Bourguès A, Noumowé A (2021) High temperature behaviour of various natural building stones. *Constr Build Mater* 272:121629
26. Masdeu F, Carmona C, Horrach G, Muñoz J (2021) Effect of iron (III) oxide powder on thermal conductivity and diffusivity of lime mortar. *Materials* 14:998
27. Shields TJ, O'Connor DJ, Silcock GWH, Donegan H (1988) Thermal bowing of a model brickwork panel. *Brick Block Mason (8th IBMAC) Lond Elsevier Appl Sci* 2:846–856
28. Zeng Q, Li K, Fen-Chong T, Dangla P (2012) Effect of porosity on thermal expansion coefficient of cement pastes and mortars. *Constr Build Mater* 28:468–475
29. Santhanam K, Ramadoss R (2022) Conservation & restoration of historic mortars at Alamparai fort with valley conical arch, Tamilnadu, India. *Constr Build Mater* 339:127619
30. Vigroux M (2020) Influence de la microstructure et de la minéralogie sur l'endommagement mécanique des pierres du patrimoine bâti sous l'effet de conditions environnementales sévères. Ph.D Thesis, Université de Cergy-Pontoise (in French)
31. Pham DT, Pinoteau N, Yang M, de Buhan P, Pimienta P, Mège R (2021) Full-scale fire test on a high-rise RC wall. *Eng Struct* 227:111435
32. Miah MJ, Pinoteau N, Pimienta P (2016) A thermo mechanical experimental investigation on 3 loaded concrete walls exposed to ISO 834-1 fire. In: Proceedings of the 9th international conference "Structures in fire"-SIF'2016, Princeton, USA
33. Franssen J-M (2005) SAFIR: a thermal/structural program for modeling structures under fire. *Eng J* 42:143–158
34. EN 1992-1-2 (2004) Eurocode 2: design of concrete structures-Part 1-2: general rules-structural fire design
35. EN 1996-1-1 (2009) Eurocode 6: design of masonry structures. Part 1-1: general rules for reinforced and unreinforced masonry structures

**Publisher's Note** Springer Nature remains neutral with regard to jurisdictional claims in published maps and institutional affiliations.

